An Efficient Synthesis of [*n*]Cycloparaphenylenes (n = 9, 12, 15) via the Self-Assembly into Macrocyclic Gold(I)-Oligophenylene Complexes Based on Dynamic Au−C σ-Bonds

Yusuke Yoshigoe,*† Yohei Tanji,† Kohtaro Osakada,§ Shinich Saito,† Yoshitaka Tsuchido,*† and Hidetoshi Kawai*†

†Department of Chemistry, Faculty of Science, Tokyo University of Science, 1–3 Kagurazaka, Shinjuku-ku, Tokyo 162-8601, Japan

§Laboratory for Chemistry and Life Science, Institute of Innovative Research, Tokyo Institute of Technology, 4259, Nagatsuta, Midori-ku, Yokohama 226-8503, Japan

ABSTRACT: The transmetalation of the digold(I) complex [Au_2Cl_2($Cy_2PCH_2PCy_2$)] with oligophenylene diboronic acids gave the triangular macrocyclic complexes [Au_2(C_6H_4)$_x$($Cy_2PCH_2PCy_2$)]$_3$ (x = 3, 4, 5) with yields of over 70%. A series of [*n*]cycloparaphenylenes (n = 9, 12, 15) was isolated in 78−88% yield *via* the oxidative chlorination of the macrocyclic gold complexes. A kinetics study employing two acyclic dinuclear gold(I) complexes, [Au_2R_2($Cy_2PCH_2PCy_2$)] (R = Ph and/or C_6H_4-4-F), revealed that an intermolecular Au(I)–C σ-bond-exchange reaction proceeded. These results indicate that the triangular complexes were obtained selectively via reversible intermolecular Au(I)–C σ-bond exchanges. By reacting two different oligophenylene diboronic acids with the digold(I) complex, a mixture of macrocyclic complexes incorporating different oligophenylene linkers was formed. The oxidative chlorination of this mixture gave [n]cycloparaphenylenes with various numbers of phenylene units.

INTRODUCTION

Cyclo[*n*]paraphenylenes ([*n*]CPPs, where *n* is the number of phenylene groups) are organic macrocycles that consist of 1,4-linked phenylene units.[1] Owing to their bent π-conjugated structure, [*n*]CPPs exhibit characteristic photo- and electrochemical properties that differ from those of linear oligophenylenes and that depend on the ring size. [2] CPPs have been widely applied in the construction of unique molecular architectures,[3] such as supramolecular host−guest molecules,[4] mechanically interlocked molecules (MIMs),[5] and building blocks for tubular nanostructures,[7] as well as in a variety of research fields, such as circularly polarized luminescent (CPL) materials,[6] biological fluorophores,[8] gas-adsorption materials,[9] and electron-transport materials.[10] The synthesis of [*n*]CPPs with a targeted ring size in high overall yield would thus be important for future applications.[11] Size-selective and shotgun syntheses of [*n*]CPPs (n = 5 − 16, 18) have been achieved by different synthetic strategies developed by Bertozzi/Jasti,[12] Itami,[13] Yamago,[14] and Osakada/Tsuchido. [15] These methods employ less-strained macrocyclic molecules or transition-metal complexes as precursors for [*n*]CPPs (Figure 1a).

In 2020, some of the authors of this paper reported the synthesis of [6]CPP from a macrocyclic Au complex (Figure 1b).[15] The reaction of 4,4′-diphenylene diboronic acid (**L2**) with [Au_2Cl_2(dcpm)] (**1**) (dcpm = bis(dicyclohexylphosphino)methane) produced the triangular hexagold(I) complex [Au_2(C_6H_4)$_2$(dcpm)]$_3$ (**Au-2**) in 77% yield. The oxidative chlorination[16] of **Au-2** by $PhICl_2$ afforded [6]CPP in a total yield of 59% (over two steps from **1**). Thus, our synthetic method has the advantage of allowing cycloparaphenylenes and related nanohoops to be synthesized from three arylene units in a highly efficient manner.[17] However, the scope of this

synthetic method using other oligophenylene derivatives, as well as the mechanism of the efficient formation of the triangular Au complexes, remain to be examined. Herein, we report the synthesis of a series of [3x]CPPs (x = 3, 4, 5) in high overall yield and in a size-selective manner from macrocyclic Au complexes with oligophenylene linkers. We have also investigated the reversible ligand exchange in acyclic arylgold(I) complexes as a model reaction for the formation of macrocyclic metal complexes. Kinetics studies of the reaction are discussed to elucidate the relevance of the dynamic behavior of the Au(I)−C bonds of the complexes to the selective and non-size-dependent formation of the macrocycles through a self-assembly process.
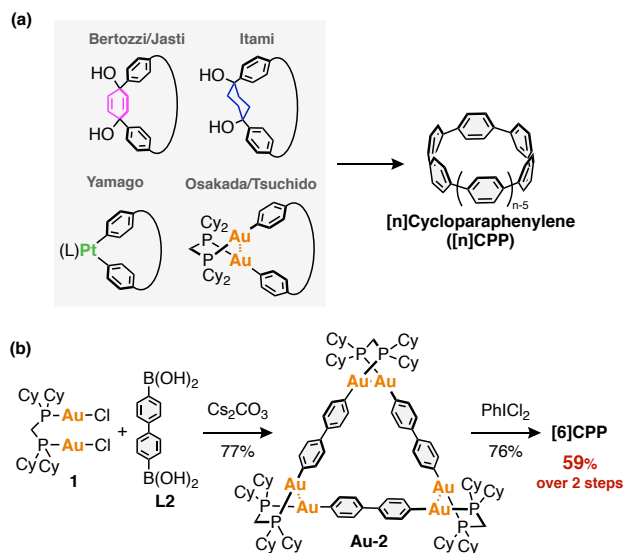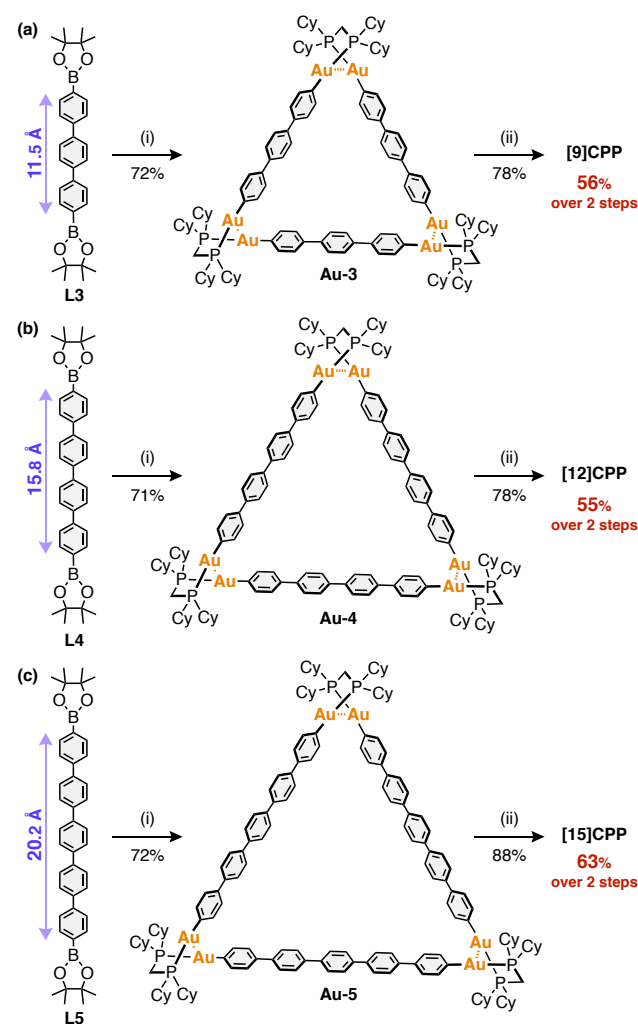
RESULTS AND DISCUSSION

Synthesis and Characterization of Au Complexes and [3*x*]CPPs. The transmetalation of [Au$_2$Cl$_2$(dcpm)] (**1**) with an equimolar amount of 4,4″-terphenylene diboronic acid pinacol ester (**L3**) was conducted in the presence of Cs$_2$CO$_3$ in toluene/ethanol/water at 50 °C. After stirring overnight, the resulting white solid was collected by filtration and characterized as the triangular macrocyclic complex [Au$_2$(C$_6$H$_4$)$_3$(dcpm)]$_3$ (**Au-3**) (Scheme 1a, reaction i). By employing oligoparaphenylene diboronic acid pinacol ester with a quaterphenylene group (**L4**) or a quinquephenylene group (**L5**) under otherwise identical reaction conditions, the corresponding Au complexes (*x* = 4 from **Au-4**, 5 from **Au-5**) were obtained in 55 and 63% yield, respectively (Scheme 1b, c, reaction i).

Scheme 1. Synthesis of [3*x*]CPP by the Au-template method. (a) [9]CPP (*x* = 3), (b) [12]CPP (*x* = 4), and (c) [15]CPP (*x* = 5). Reagents and conditions: (i) [AuCl$_2$(dcpm)] (**1**) (1.0 equiv.), Cs$_2$CO$_3$ (6.0 equiv.), toluene/ethanol/water (4:1:1), 50 °C, overnight; (ii) PhICl$_2$ (3.0 equiv.), DMF, –60 °C, 0.5 h, then r.t., overnight. Linker lengths were determined from the molecular

structures of oligophenylene simulated using MMFF force-field calculations.

Single crystals of **Au-3** (Figure 2a) and **Au-4** (Figure 2b, S42) suitable for X-ray crystallography were obtained via the vapor diffusion of CH$_3$CN into (Cl$_2$CH)$_2$ solutions of each complex. Both molecules adopt a triangular molecular structure similar to that of **Au-2**,[15] consisting of three oligophenylene linkers and three Au$_2$(dcpm) units. The complex with the terphenylene linker, **Au-3**, adopts a pseudo-*C$_2$*-symmetrical structure with *MPP*- or *PPM*-helical Au$_2$P$_2$C groups at the three corners. **Au-4** gave polymorphic crystals with a *D$_3$*-symmetrical structure and *PPP* or *MMM* helicity (Figure 2b) along with the *C$_2$*-symmetrical structure (Figure S42).[18] These triangular molecular structures were stabilized by aurophilic interactions[19] between the two Au(I) centers in each corner. In the *C$_2$*-symmetrical structure of **Au-3** (Figure 2a), the distance between the two neighboring gold atoms in one helical corner (3.297(1) Å) is longer than that of the other two corners (3.142(8), 3.118(1) Å). The same phenomenon was observed in the X-ray structures of **Au-2**[15] and **Au-4** (Figure S42) with *C$_2$*-symmetry. On the other hand, the X-ray structure of **Au-4** with *D$_3$*-symmetry (Figure 2b) exhibits Au‑Au distances of 3.091(1) Å, which are shorter than those of the *C$_2$* isomer. These results indicate stronger aurophilic interactions in the *D$_3$* isomer compared to those in the *C$_2$* isomer. Additionally, the phenylene linkers adopt a bent conformation in the *D$_3$* symmetry, which would be difficult to form with short oligophenylene linkers.
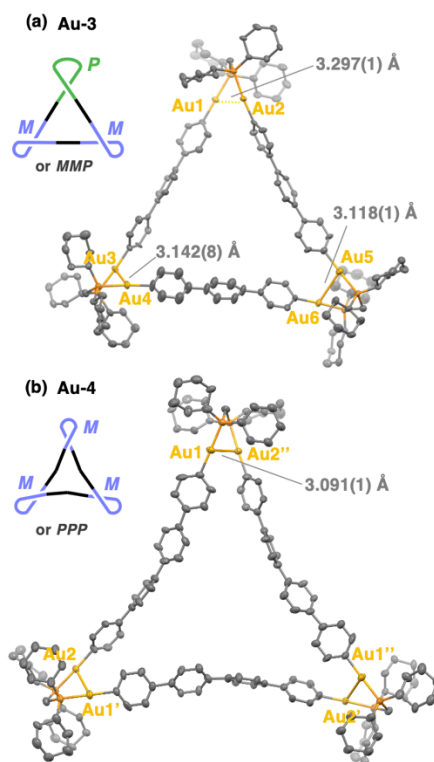

Figure 2. Molecular structures of (a) **Au-3** and (b) **Au-4** with thermal ellipsoids at 30 % probability. Hydrogen atoms and solvent molecules are omitted for clarity.

The oxidative chlorination[16] of **Au-3** occurs upon the addition of three equivalents of PhICl$_2$ in DMF at –60 °C. The C−C bond formation between two phenylene linkers via reductive elimination gave [9]CPP when the reaction temperature was raised to 25 °C (Scheme 1a, reaction ii). The ^{1}H NMR spectrum of the crude product showed only one singlet aromatic signal at 7.52 ppm (CDCl$_3$, 25 °C), which was assigned to [9]CPP based on the literature.[2] Purification of the reaction mixture using column chromatography on silica gel afforded the desired product in good yield (78%), along with the Au complex **1**, which was also obtained in 78% yield. [3x]CPPs (x = 4 for **Au-4**, 5 for **Au-5**) were obtained from the corresponding Au complexes in 78% and 88% yield, respectively (Scheme 1b, c, reactions ii). Based on our strategy, [3x]CPPs (x = 3, 4, 5) were obtained in two steps from oligophenylene diboronic acids **L3−5**. The overall yields using our methods are better than those reported by other groups (*cf.* Tables S1-S3).[20] The selective and efficient formation of the triangular complexes, which were isolated in pure form by filtration, is critical for the efficient synthesis of the CPPs, even though macrocyclization is usually a low-yield reaction. Interestingly, the macrocyclic Au complex can be selectively formed not only for the short biphenylene linker,[15] but also for the long quinquephenylene linker, for which the distance between *ipso* carbon atoms at the terminal phenylene groups is up to 20.2 Å.

Kinetics Studies of Au−C σ-Bond Exchange Reaction. Highly efficient macrocyclizations have been achieved using Pd(II) or Pt(II) complexes bound to *N*-coordinating aromatic ligands.[21] The success of these reactions has been attributed to the rapid and reversible dissociation of the linker ligands from and their re-coordination to the metal center (Scheme S2a). On the other hands, metal complexes with M-C σ-bonds such as the one used in this study hardly undergo such reversible bond-cleavage and -formation processes. However, organic transition-metal complexes, especially complexes of Pd(II) and Pt(II) with organic ligands,[22,23,24] can replace their organic ligands via reversible homonuclear transmetalation processes (Scheme S2b). We assumed that the exchange of the aryl ligands between Au(I) complexes should lead to the formation of the Au complexes **Au-3**, **Au-4**, and **Au-5**. Nevertheless, homonuclear transmetalations between two arylgold(I) complexes to exchange their aryl ligands have not been reported to date, although heteronuclear transmetalations of Au(I)–C σ bonds with Pd(II)– or Rh(I)–C σ bonds have been reported.[25-26, 28] Accordingly, we examined the dynamic bond-exchange reaction of two acyclic gold complexes to elucidate the mechanism of the efficient formation of the macrocyclic gold complexes.

We studied the aryl-group-exchange reaction between two acyclic dinuclear gold(I) complexes with different aryl groups (Figure 3a). The formation of the unsymmetrical arylgold(I) complex [Au$_2$Ph(C$_6$H$_4$-4-F)(dcpm)] (**Au$_C$-HF**) was observed upon mixing equimolar amounts (1.7 mM each) of [Au$_2$Ph$_2$(dcpm)] (**Au$_C$-HH**) and [Au$_2$(C$_6$H$_4$-4-F)$_2$(dcpm)] (**Au$_C$-FF**) in CDCl$_3$ at 25 °C. The ^{19}F NMR spectroscopic analysis indicated that the reaction reached equilibrium after 30 min (Figure 3b).[29] To our surprise, rapid bond exchange of the Au−C σ-bonds was clearly observed even at or below room temperature. The kinetic constants of the comproportionation (k_1) and disproportionation (k_{-1}) employing a mixture of **Au$_C$-HH** and **Au$_C$-FF** at -20 °C were determined to be k_1 = (6.9 ± 0.64) × 10$^-$

^{2} M^{-1}·s^{-1} and k_{-1} = (1.4 ± 0.080) × 10^{-2} M^{-1}·s^{-1} (Figure 3c). The values are in good agreement with the reversible second-order reaction model.[30] In order to understand the effect of the ancillary ligand on this surprisingly fast bond-exchange behavior, a comparative reaction was carried out with Au complexes in which the dcpm ligand was replaced by dppm (bis(diphenylphosphino)methane), **Au$_P$-HH**, and **Au$_P$-FF** (Figure 3a). As expected, the comproportionation did not occur, not even after 1 h at room temperature, suggesting that the cyclohexyl groups on the phosphines of the dcpm ligands are essential for the progress of the reaction.
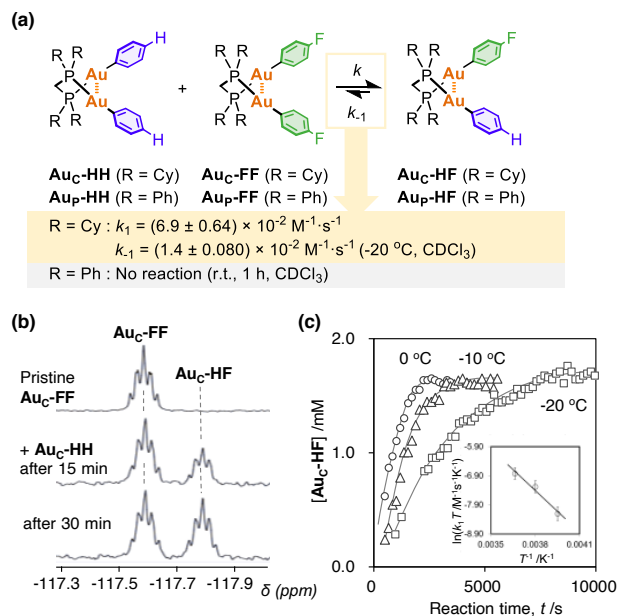

Figure 3. (a) The comproportionation of aryl ligands on Au complexes (**Au$_C$-HH** and **Au$_C$-FF**, **Au$_P$-HH** and **Au$_P$-FF**). (b) ^{19}F NMR spectra (376 MHz, CDCl$_3$, 23 °C): pristine **Au$_C$-FF** (top), a mixture of **Au$_C$-HH** and **Au$_C$-FF** 15 min after its preparation (center), and the mixture after 30 min (bottom). (c) Reaction profile of the comproportionation at 0 (circles), –10 (triangles), and –20 (squares) °C (inset: Eyring plot).

The different dynamic behavior of the arylgold(I) complexes with dcpm and dppm can be explained by comparing their crystal structures and molecular orbitals. X-ray crystallography of **Au$_C$-FF** and **Au$_P$-FF** revealed their solid-state structures (Figure 4a). The lengths of the two Au−C$_{ipso}$ bonds of **Au$_C$-FF** (2.072(4) and 2.092(5) Å) are slightly longer than those of **Au$_P$-FF** (2.062(5) Å), which suggests that the Au(I)–C σ-bonds in **Au$_C$-FF** are weaker than those in **Au$_P$-FF**. In addition, the shorter Au–P bonds of **Au$_C$-FF** (2.2903(17) and 2.2938(16) Å) compared to those of **Au$_P$-FF** (2.3013(13) Å) indicate inferior back-donation from Au to C$_{ipso}$ in **Au$_C$-FF** due to the electron-donating cyclohexyl groups. Theoretical calculations demonstrated that the lowest unoccupied molecular orbital (LUMO) of **Au$_C$-HH** is localized at the apical position of the gold atom (E = -0.737 eV), while it is delocalized to the ancillary ligand in the case of **Au$_P$-HH** (Figure 4b). The localization of the unoccupied orbital of **Au$_P$-HH** on the gold atom was observed at the LUMO+10 level (E = 0.113 eV). These results support the idea that the electrophilic gold atom of the Au complex with dcpm ligands could react with the aryl ligand.
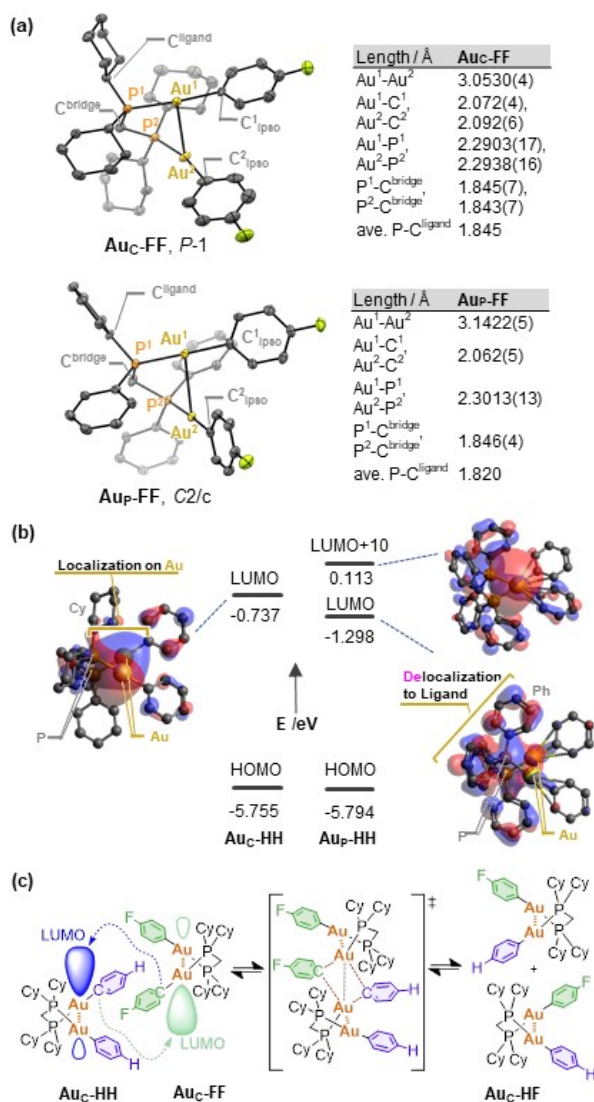
Figure 4. (a) ORTEPs of **Au$_C$-FF** and **Au$_P$-FF** with thermal ellipsoids at 50% probability; hydrogen atoms are omitted for clarity. Selected bond distances (Å) are summarized in the inserted table. (b) Energy levels of the frontier orbitals of **Au$_C$-HH** and **Au$_P$-HH** and a depiction of their LUMOs (M06/6-31G for C, H, P, LANL2TZ(f) for Au, iso value = 0.025); hydrogen atoms are omitted for clarity. (c) Proposed mechanism of the aryl-ligand-exchange reaction of the Au complex *via* an associative intermediate.

The activation parameters for the comproportionation between **Au$_C$-HH** and **Au$_C$-FF** were determined to be $\Delta G^\ddagger = 17$ kcal mol^{-1}, $\Delta H^\ddagger = 9.5$ kcal mol^{-1}, and $\Delta S^\ddagger = -26$ cal mol^{-1} K^{-1} (at 25 °C) based on the Eyring plot (Figure 3c, inset). The negative value of $\Delta S^\ddagger$ implies that the bond-exchange process proceeds *via* an associative mechanism.[22,31] We assumed that the bond exchange or metathesis between the metal centers and organic ligands should proceed *via* the formation of a four-membered C$_{aryl}$−Au−C$_{aryl}$−Au ring with an auxiliary Au-Au interaction[26,28] followed by Au−C$_{aryl}$ bond exchange to yield **Au$_C$-HF** (Figure 4c). Similar intermediates with bridging organic ligands have been proposed in kinetic studies in which arylcopper(I) and arylgold(I) complexes caused *trans–cis* isomerization of

Pd(II) complexes[25] and exchange of their aryl and alkynyl ligands bound to Pd(II) and Rh(I) complexes.[26–28]

We have previously reported the similar comproportionation of [PtPh$_2$(cod)] and [Pt(C$_6$H$_4$-4-F)$_2$(cod)] to yield the organic-ligand-exchanged complex [PtPh(C$_6$H$_4$-4-F)(cod)].[24b] These arylplatinum(II) complexes are configured as 16-electron systems, similar to the dinuclear arylgold(I) complex in this study.[32] Due to the similar reactivity of the two metal–C$_{aryl}$ bonds as well as the shared electronic nature of the metal in the above complexes, the kinetic and thermodynamic parameters of the reaction of [PtPh$_2$(cod)] were compared to that of [Au$_2$Ph$_2$(dcpm)]. In the case of [PtPh$_2$(cod)] and [Pt(C$_6$H$_4$-4-F)$_2$(cod)], the comproportionation proceeds at 50 °C with rate constants of $k_1 = (6.4 \pm 0.6) \times 10^{-6}$ and $k_2 = (2.0 \pm 0.2) \times 10^{-6}$ M^{-1} s^{-1}, which indicates slower aryl ligand exchange than in the Au$_2$ system in this study. The thermodynamic parameters for the above Pt system are $\Delta G^\ddagger = 27$ kcal mol^{-1}, $\Delta H^\ddagger = 23$ kcal mol^{-1}, and $\Delta S^\ddagger = -11$ cal mol^{-1} K^{-1}. The $\Delta H^\ddagger$ for the Pt system is larger than that for the Au$_2$ system, suggesting that the Au−C bond dissociation via the formation of the association complex can be expected to occur more easily (Figure 4c) .

These results imply that the highly efficient macrocyclization in this study should be attributed to reversible intermolecular exchanges of Au(I)–C σ-bonds (Figure 5). In the early stage of the reaction between **1** and **L3**, the formation of a mixture of acyclic and cyclic oligomers would initially proceed. The triangular complex must become the major product via the dynamic bond-exchange reaction between these species. The high thermodynamic stability and/or the poor solubility of the triangular complex could account for the isolation of the triangular complex as the sole product.
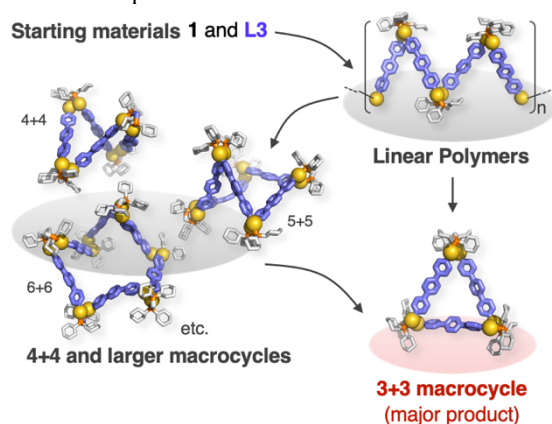

Figure 5. Illustration of a plausible mechanism for the formation of the triangular Au(I) complex **Au-3** via a self-assembly process between **1** and **L3**.

Synthesis of CPPs from two different oligophenylene linkers. To explore the scope of the potential applications of the present synthetic method, the transmetalation of [AuCl$_2$(dcpm)] (**1**) was conducted with a 1:1 mixture of two different oligophenylene diboronic acids (**L3/L4** or **L4/L5**) (Figure 6a). [33] The products gave complicated ^{1}H and ^{31}P{^{1}H} NMR spectra, which suggested the formation of mixtures of the macrocyclic gold(I) complexes with different ring sizes. Oxidation of the product by PhICl$_2$ afforded a mixture of CPPs with different ring sizes, which were characterized by comparison of their NMR spectra.

The [1H] NMR spectrum of the products obtained using an equimolar mixture of **L3** and **L4** (Figure 6b, top) contained four singlet signals that were assigned to [9], [10], [11], and [12]CPPs in a statistical ratio. The formation of the [10] and [11]CPPs as the major products indicates the formation of triangular macrocyclic complexes that incorporate two different oligophenylene linkers. No signals corresponding to other [*n*]CPPs were observed, suggesting the exclusive formation of macrocyclic hexagold(I) complexes with three linker ligands. The NMR yields of [10]CPP (1.7%) and [11]CPP (2.5%), which are CPPs derived from Au complexes with differing linkers, were slightly higher than those of [9]CPP (1.1%) and [12]CPP (1.0%), which are CPPs derived from Au complexes with identical linkers (Figure 6c). In contrast, in the **L4**/**L5** system, the yields of [12]CPP (12%) and [15]CPP (7.9%) were significantly higher than those of [13]CPP (1.0%) and [14]CPP (1.5%). This result implies that a self-sorting process occurs in the **L4**/**L5** system.

These results indicate that the Au-templated CPP synthesis outlined in this study allows the synthesis of [*n*]CPPs with numbers of phenylene units other than multiples of three via mixing two different oligophenylene linkers. The fact that the differences in the ratios of the CPP products depends on the linker length should be attributed to the thermodynamically stability of the corresponding precursor complexes. Our crystallographic study (Figure 2) revealed that macrocyclic complexes with long oligophenylene linkers can form D_3-isomers with strong aurophilic interactions, to which the self-sorting in the **L4**/**L5** system could be attributed.
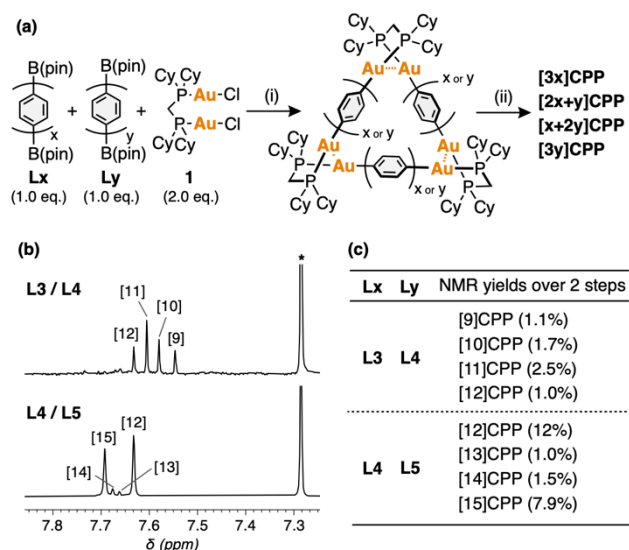

Figure 6. (a) Synthesis of [2*x*+*y*] and [*x*+2*y*]CPPs by reacting mixtures of two different oligophenylene diboronic acids, **Lx** and **Ly** (*x* = 3, *y* = 4 or *x* = 4, *y* = 5; pin = pinacol) with [AuCl$_2$(dcpm)] (**1**), followed by oxidative chlorination of the resulting complex. Reagents and conditions: (i) Cs$_2$CO$_3$ (6.0 equiv.), toluene/ethanol/water (4:1:1), 50 °C, overnight; (ii) PhICl$_2$ (3.0 equiv.), DMF, –60 °C, 0.5 h, then r.t., overnight. (b) [1H] NMR spectra of the reaction mixtures after treatment with PhICl$_2$ (400 MHz, CDCl$_3$, 25 °C). The signals were assigned with reference to reports in the literature.[2,20] The asterisk indicates the residual solvent signal. (c) List of NMR yields of the CPPs over 2 steps. The NMR yields were determined from the

[1H] signal intensities relative to an internal standard (1,2,4,5-tetrabromobenzene).

CONCLUSIONS

We have demonstrated the highly efficient self-assembly of triangular macrocyclic Au complexes, [Au$_2$(C$_6$H$_4$)$_x$(Cy$_2$PCH$_2$PCy$_2$)]$_3$ (*x* = 3, 4, 5), which were obtained from the transmetalation of [Au$_2$Cl$_2$(Cy$_2$PCH$_2$PCy$_2$)] with oligophenylene diboronic acids. The chemical oxidation of the complexes produced the corresponding [3*x*]cyclopara-phenylenes ([3*x*]CPPs) (*x* = 3, 4, 5) in good yields. Kinetics studies of the acyclic Au$_2$ complexes [Au$_2$R$_2$(Cy$_2$PCH$_2$PCy$_2$)] (R = Ph and/or C$_6$H$_4$-4-F) revealed that the intermolecular transmetalation of the aryl ligands proceeds with low activation energy, which would explain the high efficiency of the macrocyclization via the thermodynamically controlled self-assembly process. We have also demonstrated that the reaction of two different oligophenylene diboronic acids with the digold(I) complex resulted in the formation of a mixture of triangular macrocyclic complexes that incorporate different oligophenylene linkers, which produced [2*x*+*y*] and [*x*+2*y*]CPPs together with [3*x*] and [3*y*]CPPs (*x* = 3, *y* = 4 or *x* = 4, y = *5*). The concise synthetic strategy outlined in this study allows facile access to a variety of [*n*]CPPs in high overall yield. Our method thus provides a new pathway for the synthesis of a variety of functionalized CPPs and related nanohoops.[35] The synthesis of [3*x*]CPPs (*x* > 5) from macrocyclic Au(I) complexes with oligophenylene linkers longer than those in this study is currently in progress.

ASSOCIATED CONTENT

The Supporting Information is available free of charge at https://pubs.acs.org/doi/xxxxxxxx.

Experimental procedures, NMR spectra, theoretical studies, and X-ray crystallography data (PDF, CIF)

Accession Codes

CCDC 2108728 (**Au-3**), 2108731 (**Au-4 D_3**), 2108730 (**Au-4 C_2**), 2108732 (**Au$_C$-FF**), 2108733 (**Au$_P$-FF**), and 2108729 (**Au$_C$-HH**) contain the supplementary crystallographic data for this paper. These data can be obtained free of charge via www.ccdc.cam.ac.uk/data_request/cif, or by emailing data_request@ccdc.cam.ac.uk, or by contacting The Cambridge Crystallographic Data Centre, 12 Union Road, Cambridge CB2 1EZ, UK; fax: +44 1223 336033.

AUTHOR INFORMATION

Corresponding Authors

Yusuke Yoshigoe - *Department of Chemistry, Faculty of Science, Tokyo University of Science, 1–3 Kagurazaka, Shinjuku-ku, Tokyo 162-8601, Japan,* http://orcid.org/0000-0003-0869-9509; Email: yoshigoe.yusuke@rs.tus.ac.jp

Yoshitaka Tsuchido - *Department of Chemistry, Faculty of Science, Tokyo University of Science, 1–3 Kagurazaka, Shinjuku-ku, Tokyo 162-8601, Japan,* http://orcid.org/0000-0001-8860-0745; Email: tsuchido@rs.tus.ac.jp

Hidetoshi Kawai - *Department of Chemistry, Faculty of Science, Tokyo University of Science, 1–3 Kagurazaka, Shinjuku-ku, Tokyo*

162-8601, Japan, http://orcid.org/0000-0002-3367-0153; Email: kawaih@rs.tus.ac.jp

Authors

Yohei Tanji - *Graduate School of Science, Tokyo University of Science, 1–3 Kagurazaka, Shinjuku-ku, Tokyo 162-8601, Japan*

Shinichi Saito - *Department of Chemistry, Faculty of Science, Tokyo University of Science, 1–3 Kagurazaka, Shinjuku-ku, Tokyo 162-8601, Japan,* http://orcid.org/0000-0001-8520-1116

Kohtaro Osakada - *Laboratory for Chemistry and Life Science, Institute of Innovative Research, Tokyo Institute of Technology, 4259, Nagatsu-ta, Midori-ku, Yokohama 226-8503, Japan,* http://orcid.org/0000-0003-0538-9978

Notes

The authors declare no conflicts of interest.

REFERENCES

[1] (a) Yamago, S.; Kayahara, E.; Iwamoto, T. Organoplatinum-Mediated Synthesis of Cyclic π-Conjugated Molecules: Towards a New Era of Three-Dimensional Aromatic Compounds. *Chem. Rec.* **2014**, *14*, 84–100; (b) Golder, M. R.; Jasti, R. Syntheses of the Smallest Carbon Nanohoops and the Emergence of Unique Physical Phenomena. *Acc. Chem. Res.* **2015**, *48*, 557–566; (c) Segawa, Y.; Yagi, A.; Matsui, K.; Itami, K. Design and Synthesis of Carbon Nanotube Segments. *Angew. Chem., Int. Ed.* **2016**, *55*, 5136–5158; (d) Yamago, S.; Kayahara, E. Synthesis and Reactions of Carbon Nanohoop. *J. Synth. Org. Chem.* **2019**, *77*, 1147–1158.

[2] Darzi, E. R.; Jasti, R. The Dynamic, Size-Dependent Properties of [5]-[12]Cycloparaphenylenes. *Chem. Soc. Rev.* **2015**, *44*, 6401–6410.

[3] (a) Xu, Y.; von Delius, M. The Supramolecular Chemistry of Strained Carbon Nanohoops. *Angew. Chem., Int. Ed.* **2020**, *59*, 559–573; (b) Hermann, M.; Wassy, D.; Esser, B. Conjugated Nanohoops Incorporating Donor, Acceptor, Hetero- or Polycyclic Aromatics. *Angew. Chem., Int. Ed.* **2020**, 60, 15743–15766; (c) Mirzaei, S.; Castro, E.; Hernández Sánchez, R. Conjugated Molecular Nanotubes. *Chem. − Eur. J.* **2021**, *27*, 8642–8655.

[4] (a) Iwamoto, T.; Watanabe, Y.; Sadahiro, T.; Haino, T.; Yamago, S. Size-Selective Encapsulation of C$_{60}$ by [10]Cycloparaphenylene: Formation of the Shortest Fullerene-Peapod. *Angew. Chem., Int. Ed.* **2011**, *50*, 8342–8344; (b) Hashimoto, S.; Iwamoto, T.; Kurachi, D.; Kayahara, E.; Yamago, S. Shortest Double-Walled Carbon Nanotubes Composed of Cycloparaphenylenes. *ChemPlusChem* **2017**, *82*, 1015–1020; (c) Matsuno, T.; Fujita, M.; Fukunaga, K.; Sato, S.; Isobe, H. Concyclic CH-π Arrays for Single-Axis Rotations of a Bowl in a Tube. *Nat. Commun.* **2018**, *9*, 3779; (d) Della Sala, P.; Talotta, C.; Caruso, T.; De Rosa, M.; Soriente, A.; Neri, P.; Gaeta, C. Tuning Cycloparaphenylene Host Properties by Chemical Modification. *J. Org. Chem.* **2017**, *82*, 9885–9889; (e) Lu, D.; Zhuang, G.; Jia, H.; Wang, J.; Huang, Q.; Cui, S.; Du, P. A Novel Symmetrically Multifunctionalized Dodecamethoxy-Cycloparaphenylene: Synthesis, Photophysical, and Supramolecular Properties. *Org. Chem. Front.* **2018**, *5*, 1446–1451; (f) Cui, S.; Zhuang, G.; Wang, J.; Huang, Q.; Wang, S.; Du, P. Multifunctionalized Octamethoxy-[8]Cycloparaphenylene: Facile Synthesis and Analysis of Novel Photophysical and Photoinduced Electron Transfer Properties. *Org. Chem. Front.* **2019**, *6*, 1885–1890; (g) Lu, D.; Huang, Q.; Wang, S.; Wang, J.; Huang, P.; Du, P. The Supramolecular

Chemistry of Cycloparaphenylenes and Their Analogs. *Front. Chem.* **2019**, *7*, 668.

[5] (a) Xu, Y.; Kaur, R.; Wang, B.; Minameyer, M. B.; Gsänger, S.; Meyer, B.; Drewello, T.; Guldi, D. M.; Von Delius, M. Concave-Convex π-π Template Approach Enables the Synthesis of [10]Cycloparaphenylene-Fullerene [2]Rotaxanes. *J. Am. Chem. Soc.* **2018**, *140*, 13413–13420; (b) Van Raden, J. M.; White, B. M.; Zakharov, L. N.; Jasti, R. Nanohoop Rotaxanes from Active Metal Template Syntheses and Their Potential in Sensing Applications. *Angew. Chem., Int. Ed.* **2019**, *58*, 7341–7345; (c) Segawa, Y.; Kuwayama, M.; Hijikata, Y.; Fushimi, M.; Nishihara, T.; Pirillo, J.; Shirasaki, J.; Kubota, N.; Itami, K. Topological Molecular Nanocarbons: All-Benzene Catenane and Trefoil Knot. *Science* **2019**, *365*, 272–276.

[6] (a) Hitosugi, S.; Nakanishi, W.; Yamasaki, T.; Isobe, H. Bottom-up Synthesis of Finite Models of Helical (n,m)-Single-Wall Carbon Nanotubes. *Nat. Commun.* **2011**, *2*, 8–12; (b) Nogami, J.; Tanaka, Y.; Sugiyama, H.; Uekusa, H.; Muranaka, A.; Uchiyama, M.; Tanaka, K. Enantioselective Synthesis of Planar Chiral Zigzag-Type Cyclophenylene Belts by Rhodium-Catalyzed Alkyne Cyclotrimerization. *J. Am. Chem. Soc.* **2020**, *142*, 9834–9842; (c) Nogami, J.; Nagashima, Y.; Miyamoto, K.; Muranaka, A.; Uchiyama, M.; Tanaka, K. Asymmetric Synthesis, Structures, and Chiroptical Properties of Helical Cycloparaphenylenes. *Chem. Sci.* **2021**, *12*, 7858–7865; (d) Sato, K.; Hasegawa, M.; Nojima, Y.; Hara, N.; Nishiuchi, T.; Imai, Y.; Mazaki, Y. Circularly Polarized Luminescence of a Stereogenic Curved Paraphenylene Anchoring a Chiral Binaphthyl in Solution and Solid State. *Chem. − Eur. J.* **2021**, *27*, 1323–1329.

[7] (a) Omachi, H.; Nakayama, T.; Takahashi, E.; Segawa, Y.; Itami, K. Initiation of Carbon Nanotube Growth by Well-Defined Carbon Nanorings. *Nat. Chem.* **2013**, *5*, 572–576; (b) Ozaki, N.; Sakamoto, H.; Nishihara, T.; Fujimori, T.; Hijikata, Y.; Kimura, R.; Irle, S.; Itami, K. Electrically Activated Conductivity and White Light Emission of a Hydrocarbon Nanoring–Iodine Assembly. *Angew. Chem., Int. Ed.* **2017**, *56*, 11196–11202; (c) Leonhardt, E. J.; Van Raden, J. M.; Miller, D.; Zakharov, L. N.; Alemán, B.; Jasti, R. A Bottom-Up Approach to Solution-Processed, Atomically Precise Graphitic Cylinders on Graphite. *Nano Lett.* **2018**, *18*, 7991–7997; (d) Huang, Q.; Zhuang, G.; Zhang, M.; Wang, J.; Wang, S.; Wu, Y.; Yang, S.; Du, P. A Long π-Conjugated Poly(para-Phenylene)-Based Polymeric Segment of Single-Walled Carbon Nanotubes. *J. Am. Chem. Soc.* **2019**, *141*, 18938–18943.

[8] (a) Tang, H.; Gu, Z.; Li, C.; Li, Z.; Wu, W.; Jiang, X. Nanoscale Vesicles Assembled from Non-Planar Cyclic Molecules for Efficient Cell Penetration. *Biomater. Sci.* **2019**, *7*, 2552–2558; (b) White, B. M.; Zhao, Y.; Kawashima, T. E.; Branchaud, B. P.; Pluth, M. D.; Jasti, R. Expanding the Chemical Space of Biocompatible Fluorophores: Nanohoops in Cells. *ACS Cent. Sci.* **2018**, *4*, 1173–1178.

[9] (a) Sakamoto, H.; Fujimori, T.; Li, X.; Kaneko, K.; Kan, K.; Ozaki, N.; Hijikata, Y.; Irle, S.; Itami, K. Cycloparaphenylene as a Molecular Porous Carbon Solid with Uniform Pores Exhibiting Adsorption-Induced Softness. *Chem. Sci.* **2016**, *7*, 4204–4210; (b) Frydrych, R.; Lis, T.; Bury, W.; Cybińska, J.; Stępień, M. Feeding a Molecular Squid: A Pliable Nanocarbon Receptor for Electron-Poor Aromatics. *J. Am. Chem. Soc.* **2020**, *142*, 15604–15613; (c) Schaub, T. A.; Prantl, E. A.; Kohn, J.; Bursch, M.; Marshall, C. R.; Leonhardt, E. J.; Lovell, T. C.; Zakharov, L. N.; Brozek, C. K.; Waldvogel, S. R.; Grimme, S.; Jasti, R. Exploration of the Solid-State Sorption Properties of Shape-Persistent Macrocyclic Nanocarbons as Bulk Materials and Small Aggregates. *J. Am. Chem. Soc.* **2020**, *142*, 8763–8775.

[10] Kayahara, E.; Sun, L.; Onishi, H.; Suzuki, K.; Fukushima, T.; Sawada, A.; Kaji, H.; Yamago, S. Gram-Scale Syntheses and Conductivities of [10]Cycloparaphenylene and Its Tetraalkoxy Derivatives. *J. Am. Chem. Soc.* **2017**, *139*, 18480–18483.

[11] Leonhardt, E. J.; Jasti, R. Emerging applications of carbon nanohoops. *Nat. Rev. Chem.* **2019**, *3*, 672–686.

[12] Jasti, R.; Bhattacharjee, J.; Neaton, J. B.; Bertozzi, C. R. Synthesis, Characterization, and Theory of [9]-, [12]-, and [18]Cycloparaphenylene: Carbon Nanohoop Structures. *J. Am. Chem. Soc.* **2008**, *130*, 17646–17647.

[13] Takaba, H.; Omachi, H.; Yamamoto, Y.; Bouffard, J.; Itami, K. Selective Synthesis of [12]Cycloparaphenylene. *Angew. Chem., Int. Ed.* **2009**, *48*, 6112–6116.

[14] Yamago, S.; Watanabe, Y.; Iwamoto, T. Synthesis of [8]Cyclo-paraphenylene from a Square-Shaped Tetranuclear Platinum Complex. *Angew. Chem., Int. Ed.* **2010**, *49*, 757–759.

[15] Tsuchido, Y.; Abe, R.; Ide, T.; Osakada, K. A Macrocyclic Gold(I)–Biphenylene Complex: Triangular Molecular Structure with Twisted Au$_2$(Diphosphine) Corners and Reductive Elimination of [6]Cycloparaphenylene. *Angew. Chem., Int. Ed.* **2020**, *59*, 22928–22932.

[16] Wolf, W. J.; Winston, M. S.; Toste, F. D. Exceptionally Fast Carbon-Carbon Bond Reductive Elimination from Gold(III). *Nat. Chem.* **2014**, *6*, 159–164.

[17] By employing Yamago's Pt method, [3*x*]CPP derivatives were obtained by applying an arylene linker with a bent structure or a long oligoarylene linker, and the corresponding [4*x*]CPP derivatives were also obtained. The structurally stressed or flexible organic linker would reduce the thermal stability of the square-shaped Pt$_4$ complex, which allows the formation of a triangular Pt$_3$ complex. (a) Kayahara, E.; Qu, R.; Kojima, M.; Iwamoto, T.; Suzuki, T.; Yamago, S. Ligand-Controlled Synthesis of [3]- and [4]Cyclo-9,9-Dimethyl-2,7-Fluorenes through Triangle- and Square-Shaped Platinum Intermediates. *Chem.–Eur. J.* **2015**, *21*, 18939–18943; (b) Kogashi, K.; Matsuno, T.; Sato, S.; Isobe, H. Narrowing Segments of Helical Carbon Nanotubes with Curved Aromatic Panels. *Angew. Chem., Int. Ed.* **2019**, *58*, 7385–7389; (c) Zhao, H.; Cao, L.; Huang, S.; Ma, C.; Chang, Y.; Feng, K.; Zhao, L.-L.; Zhao, P.; Yan, X. Synthesis, Structure, and Photophysical Properties of *m*-Phenylene-Embedded Cycloparaphenylene Nanorings. *J. Org. Chem.* **2020**, *85*, 6951–6958; (d) Ikemoto, K.; Fujita, M.; Too, P. C.; Tnay, Y. L.; Sato, S.; Chiba, S.; Isobe, H. Synthesis and Structures of π-Extended [*n*]Cyclo-*para*-Phenylenes (n = 12, 16, 20) Containing *n*/2 Nitrogen Atoms. *Chem. Lett.* **2016**, *45*, 658–660; (e) Jia, H.; Zhuang, G.; Huang, Q.; Wang, J.; Wu, Y.; Cui, S.; Yang, S.; Du, P. Synthesis of Giant π-Extended Molecular Macrocyclic Rings as Finite Models of Carbon Nanotubes Displaying Enriched Size-Dependent Physical Properties. *Chem.–Eur. J.* **2020**, *26*, 2159–2163.

[18] We also obtained the X-ray structure of polymorphic **Au-4** with C_2-symmetry using the structure-analysis tool "What Is This" (Figure S42). Matsumoto, T.; Yamano, A.; Sato, T.; Ferrara, J. D.; White, F. J.; Meyer, M. "What Is This?" A Structure Analysis Tool for Rapid and Automated Solution of Small Molecule Structures. *J. Chem. Crystallogr.* **2020**, *51*, 438–450.

[19] (a) Schmidbaur, H. Ludwig Mond Lecture. High-carat Gold Compounds. *Chem. Soc. Rev.* **1995**, *24*, 391–400; (b) Schmidbaur, H. The Aurophilicity Phenomenon: A Decade of Experimental Findings, Theoretical Concepts and Emerging Applications. *Gold Bull.* **2000**, *33*, 3–10; (c) Schmidbaur, H.; Schier, A. A Briefing on Aurophilicity. *Chem. Soc. Rev.* **2008**, *37*, 1931–1951; (d) Schmidbaur, H.; Schier, A. Aurophilic Interactions as a Subject of Current Research: An Up-Date. *Chem. Soc. Rev.* **2012**, *41*, 370–412.

[20] Omachi, H.; Matsuura, S.; Segawa, Y.; Itami, K. A Modular and Size-Selective Synthesis of [n]Cycloparaphenylenes: A Step toward the Selective Synthesis of [n,n] Single-Walled Carbon Nanotubes. *Angew. Chem., Int. Ed.* **2010**, *49*, 10202–10205.

[21] (a) Fujita, M.; Tominaga, M.; Hori, A.; Therrien, B. Coordination Assemblies from a Pd(II)-Cornered Square Complex. *Acc. Chem. Res.* **2005**, *38*, 369–378; (b) Sun, Y.; Chen, C.; Liu, J.; Stang, P. J. Recent Developments in the Construction and Applications of Platinum-Based Metallacycles and Metallacages: Via Coordination. *Chem. Soc. Rev.* **2020**, *49*, 3889–3919; (c) Hiraoka, S.; Takahashi, S.; Sato, H. Coordination Self-Assembly Processes Revealed by Collaboration of Experiment and Theory: Toward Kinetic Control of Molecular Self-Assembly. *Chem. Rec.* **2021**, *21*, 443–459.

[22] (a) Casado, A. L. Casares, J. A.; Espinet, P. An Aryl Exchange Reaction with Full Retention of Configuration of the Complexes: Mechanism of the Aryl Exchange between [PdR$_2$L$_2$] Complexes in Chloroform (R = Pentahalophenyl, L = Thioether). *Organometallics* **1997**, *16*, 5730-5736; (b) Casado, A L.; Casares, A.; Espinet, P. Mechanism of the Uncatalyzed Dissociative Cis−Trans Isomerization of

Bis(pentafluorophenyl)bis(tetrahydrothiophene): A Refinement. *Inorg. Chem.* **1998**, *37*, 4154–4156.

[23] Ozawa, F.; Ito, T.; Nakamura, Y.; Yamamoto, A. Mechanism of Thermal Decomposition of *trans*- and *cis*-Dialkylbis(tertiary phosphine)palladium(II). Reductive Elimination and trans to cis Isomerization. *Bull. Chem. Soc. Jpn.*, **1981**, *54*, 1868–1880.

[24] (a) Suzaki, Y.; Yagyu, T.; Yamamura, Y.; Mori, A.; Osakada, K. Disproportionation of PtPh(CH$_2$COMe)(cod) and Conproportionation of PtPh$_2$(cod) and Pt(CH$_2$COMe)$_2$(cod) via Intermolecular Phenyl Ligand Transfer. *Organometallics* **2002**, *21*, 5254-5258. (b) Yoshigoe, Y.; Suzaki, Y.; Osakada, K. Intermolecular Aryl Ligands Transfer of the Diarylplatinum(II) Complexes with a Cyclooctadiene Ligand. *Chem. Lett.* **2014**, *43*, 1337–1339.

[25] Casado, A. L.; Espinet, P. A Novel Reversible Aryl Exchange Involving Two Organometallics: Mechanism of the Gold(I)-Catalyzed Isomerization of *trans*-[PdR$_2$L$_2$] Complexes (R = Aryl, L = SC$_4$H$_8$). *Organometallics* **1998**, *17*, 3677–3683.

[26] (a) Peñas-Defrutos, M. N.; Bartolomé, C.; García-Melchor, M.; Espinet, P. Rh^{I}Ar/Au^{I}Ar Transmetalation: A Case of Group Exchange Pivoting on the formation of M–M' Bonds through Oxidative Insertion. *Angew. Chem., Int. Ed.* **2019**, *58*, 3501–3505. (b) Villar, P.; Pérez-Temprano, M. H.; Casares, J. A.; Álavarez, R.; Espinet, P. Experimental and DFT Study of the [AuAr(AsPh$_3$)]-Catalyzed *cis/trans* Isomerization of [PdAr$_2$(AsPh$_3$)$_2$] (Ar = C$_6$F$_5$ or C$_6$Cl$_2$F$_3$): Alternative Mechanisms and its Switch upon Pt for Pd Substitution. *Organometallics* **2020**, *39*, 2295–2303.

[27] For a arylcopper(I)-palladium ligand transfer, i.e., the analogous reaction of a Pd(II) complex and an arylcopper(I) complex, which have group-11 metals in common and the same electronic configuration as arylgold(II) complexes, see: Pérez-Iglesias, M.; Lozano-Lavilla, O.; Casares, J. A. [Cu(C$_6$Cl$_2$F$_3$)(tht)]$_4$: An Extremely Efficient Catalyst for the Aryl Scrambling between Palladium Complexes. *Organometallics* **2019**, *38*, 739−742.

[28] For a reaction involving alkynyl-ligand transfer between Au(I) and Pd(II), see: (b) Toledo, A.; Meana, I.; Albéniz, A. C. Formal Gold-to-Gold Transmetalation of an Alkynyl Group Mediated by Palladium: A Bisalkynyl Gold Complex as a Ligand to Palladium. *Chem. – Eur. J.* **2015**, *21*, 13216–13220.

[29] The concentrations of the Au complexes were determined based on a comparison of the ^{19}F and ^{1}H NMR peak areas of these complexes with that of the internal standard 1,3,5-tris(trifluoromethyl)benzene (^{19}F NMR: δ -63.5; ^{1}H NMR: δ -63.5); or further details, see the Supporting Information.

[30] Szabó, Z. G. Comprehensive Chemical Kinetics vol 2.; Bamford, C. H. and Tipper, C. H. F. Eds.; Elsevier: Amsterdam, 1969; Chapter 1, Kinetic Characterization of Complex Reaction System, p 43.

[31] Carbon-bridged bimetallic complexes were isolated and these are known as a key intermediate of transmetalation reactions; for details, see also references listed in ref. 22.

[32] [PtPh$_2$(cod)] is a 16-electron complex of platinum(II) with a d_8 electronic configuration, which contains two Pt−C$_{aryl}$ σ-bonds and two Pt-(C=C) π-coordination bonds. [Au$_2$Ph$_2$(dcpm)] is a 16-electron complex of two gold(I) atoms, in which both gold atoms have a d_{10} electronic configuration and contain an Au−C$_{aryl}$ σ-bond, an Au−P coordination bond, and an Au−Au interaction.

[33] (a) Iwamoto, T.; Watanabe, Y.; Sakamoto, Y.; Suzuki, T.; Yamago, S. Selective and Random Syntheses of [*n*]Cycloparaphenylenes (*n* = 8-13) and Size Dependence of Their Electronic Properties. *J. Am. Chem. Soc.* **2011**, *133*, 8354–8361; (b) Fukunaga, T. M.; Sawabe, C.; Matsuno, T.; Takeya, J.; Okamoto, T.; Isobe, H. Manipulations of Chiroptical Properties in Belt-persistent Cycloarylenes via Desymmetrization with Heteroatom Doping. *Angew. Chem., Int. Ed.* **2021**, *60*, 19097−19101.

[33] (a) Lehn, J.-M. Perspectives in Chemistry−Steps towards Complex Matter. *Angew. Chem., Int. Ed.* **2013**, *52*, 2836–2850; (b) Zheng, Y.-R.; Yang, H.-B.; Northrop, B. H.; Ghosh, K.; Stang, P. J. Size Selective Self-Sorting in Coordination-Driven Self-Assembly of Finite Ensembles. *Inorg. Chem.* **2008**, *47*, 4706–4711; (c) Bunzen, J.; Iwasa, J.; Bonakdarzadeh, P.; Numata, E.; Rissanen, K.; Sato, S.; Fujita, M. Self-Assembly of M$_{24}$L$_{48}$ Polyhedra Based on Empirical Prediction. *Angew.*

Chem., Int. Ed. **2012**, *51*, 3161–3163; (d) Tateishi, T.; Kojima, T.; Hiraoka, S. Chiral Self-Sorting Process in the Self-Assembly of Homochiral Coordination Cages from Axially Chiral Ligands. *Commun. Chem.* **2018**, *1*, 20; (e) Rizzuto, F. J.; Nitschke, J. R. Narcissistic, Integrative, and Kinetic Self-Sorting within a System of Coordination Cages. *J. Am. Chem. Soc.* **2020**, *142*, 7749–7753.

[34] Qiu, Z.-L.; He, M.-b.; Chu, K.-S.; Tang, C.; Chen, X.-W.; Zhu, L.; Zhang, L.-P.; Sun, D.; Qian, J.; Tan, Y.-Z. Well-Defined Segment of Carbon Nanotube with Bright Red Emission for Three-Photon Fluorescence Cerebrovascular Imaging. *Adv. Optical Mater.* **2021**, *in press*, doi.org/10.1002/adom.202100482.

Insert Table of Contents artwork here